



Exploring the UDP pocket of LpxC through amino acid analogs



Michael R. Hale*, Pamela Hill, Sushmita Lahiri, Matthew D. Miller, Philip Ross, Richard Alm, Ning Gao, Amy Kutschke, Michele Johnstone, Bryan Prince, Jason Thresher, Wei Yang

Infection Innovative Medicines Unit, AstraZeneca R&D Boston, 35 Gatehouse Drive, Waltham, MA 02451, USA

ARTICLE INFO

Article history:

Received 16 November 2012

Revised 6 February 2013

Accepted 12 February 2013

Available online 1 March 2013

Keywords:

LpxC

Inhibitor

Antibiotic

Hydroxamate

ABSTRACT

Lipopolysaccharide (LPS) biosynthesis is an attractive antibacterial target as it is both conserved and essential for the survival of key pathogenic bacteria. Lipid A is the hydrophobic anchor for LPS and a key structural component of the outer membrane of Gram-negative bacteria. Lipid A biosynthesis is performed in part by a unique zinc dependent metalloamidase, LpxC (UDP-3-O-(R-3-hydroxymyristoyl)-N-acetylglucosamine deacetylase), which catalyzes the first non-reversible step in lipid A biosynthesis. The UDP portion of the LpxC substrate-binding pocket has been relatively unexplored. We have designed and evaluated a series of hydroxamate based inhibitors which explore the SAR of substitutions directed into the UDP pocket with a range of substituted α -amino acid based linkers. We also provide the first wild type structure of *Pseudomonas aeruginosa* LpxC which was utilized in the design of many of these analogs.

© 2013 Elsevier Ltd. All rights reserved.

There is a critical need for discovery of novel agents targeting Gram-negative bacteria as there is a rising incidence of resistance to existing therapies.¹ Additionally, new agents are not being developed fast enough to rebuild our arsenal of treatments. The composition of the outer membrane includes lipopolysaccharide (LPS) providing a charged layer to protect the cells from the passive entry of hydrophobic agents including antibiotics.² Getting through this protective outer membrane is one of the challenges in targeting Gram-negative bacteria. The inner membrane of Gram-negative bacteria provides a more lipophilic barrier; inhibitors must maintain a balance of physical properties to penetrate both membranes effectively.

LpxC is an attractive target as it is the first non-reversible step in the synthesis of lipid A, the hydrophobic anchor for LPS present in the leaflet of the outer membrane of Gram-negative bacteria.³ The lipid A biochemical pathway has recently become an important target for Gram-negative antibacterial drug discovery.⁴ Lipid A is made on the inner side of the cytosolic membrane by a cascade of enzymes including LpxC.⁵ After synthesis, lipid A is transported to the extracellular side of the outer membrane. LpxC has been determined to be essential, as failure of bacteria to produce lipid A results in inhibition of bacterial growth and cell death.⁶ Recently there have been reports of the in vivo validation of LpxC as a drug target.⁷ LpxC inhibitors could be utilized in the treatment of clinical indications where Gram-negative pathogens predominate. Clinical indications such as urinary tract, intra-abdominal infections as well as hospital acquired pneumonia are predominated

by the following pathogens; *Pseudomonas aeruginosa*, *Escherichia coli*, *Klebsiella pneumoniae*.

LpxC contains an active site zinc ion which is required for catalyzing the deacetylation of UDP-3-O-(R-3-hydroxymyristoyl)-N-acetylglucosamine. There have been numerous reports of hydroxamate based inhibitors that have been effective at binding LpxC through coordination to the active site Zn.⁸ The active site zinc in both *P. aeruginosa* and *E. coli* LpxC has an atypical binding motif, bound by two histidines and an aspartic acid which may be beneficial in providing inhibitors with selectivity over other Zn²⁺ dependent enzymes. Additionally the secondary structure of the protein is a typical, a β - α - α - β sandwich fold where four α helices are held between two β sheets, which could contribute to additional selectivity.⁹

Design: A series of inhibitors as shown in Figure 1 were designed and synthesized to evaluate the SAR of analogs with diversity at R¹ and to compare activities to CH-12.¹⁰ CH-12 is an LpxC inhibitor disclosed by Chiron and is used as a comparator in this effort. CH-90¹¹ is one of the more potent and widely used comparators for LpxC inhibitors in which there are now numerous examples. The initial compounds were designed and prioritized based on a *P. aeruginosa* LpxC homology model. The goal of the design set was to evaluate diversity at R¹ through a series of amino acid based linkers and study the impact on enzymatic potency, physical properties and target accessibility (Fig. 1).

Many Zn dependant enzymes including LpxC have similar pharmacophores. The catalytic Zn is coordinated to the warhead, a hydroxamate in this case. The warhead can also bind to active site residues. The warhead is quite often linked to a core that is substituted by a hydrophobic tail and in some cases additional

* Corresponding author. Tel.: +1 781 839 4113; fax: +1 781 839 4630.

E-mail address: michael.hale@astrazeneca.com (M.R. Hale).

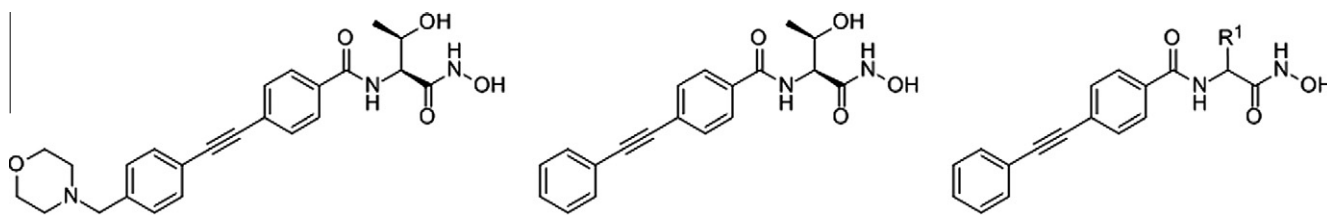
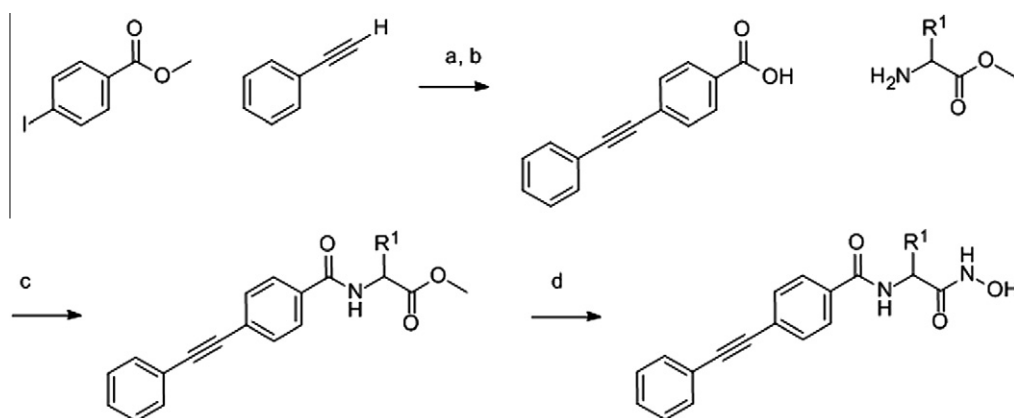


Figure 1. CH-90, CH-12, generic for R¹ library diversity.



Scheme 1. Description of general route. Reagents and conditions: (a) Sonagashira conditions, (b) HATU coupling conditions, (c) 50% aq. Hydroxylamine, MeOH, rt 12 h.

substitution into what is referred to as the UDP pocket in LpxC. The inhibitors discussed in this Letter focus on diversity in the UDP pocket through R¹ variations, we then studied how they impact potency. The differences in R¹ sizes, properties and geometry can be used to design selective inhibitors and enhance potency for LpxC.

The synthesis of the compounds evaluated is outlined generically in Scheme 1. The phenylacetylene benzoic acid is first assembled through a Sonagashira coupling. This is followed by a HATU mediated coupling and the introduction of a series of α -amino acids. The final step is conversion to the hydroxamic acid which is accomplished using 50% aqueous hydroxylamine in methanol. In some cases the intermediate ester was modified prior to hydroxamic acid formation.

The plan was to vary the substitution and chirality by incorporating a series of natural and unnatural α -amino acids as linkers and to evaluate the impact of R¹ on enzymatic and cellular potency. The compounds were evaluated for enzymatic inhibition (IC₅₀), wild type (WT) and efflux pump deficient (PD) MIC values in both *P. aeruginosa* (WT: Pae545 and PD: Pae546), and *E. coli* (WT: Eco523 and PD: Eco524), as well as being evaluated for changes in physical properties (AZ Log D and plasma protein binding).^{12,13} AZ Log is a modified algorithm for calculation of lipophilicity developed at AstraZeneca.¹⁴

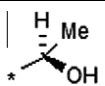
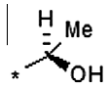
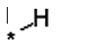
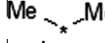
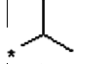
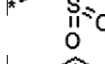
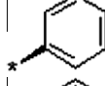
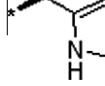
For an initial evaluation of the series we made the glycine based analog and compared the properties to the *s,s*-threonine compound bearing the same hydrophobic substituent, the diphenylacetylene (CH-12), see Table 1. A second important comparison was the extension of the hydrophobic group where it can interact with solvent and perhaps improve physical properties, CH-90 (Fig. 1). CH-12 does not probe deeply into the UDP portion of the active site. The series of compounds described here was designed to evaluate potential for improved binding through extension of the R¹ into the phosphate and ribose binding region of the UDP pocket. As shown in Table 1, the length of the substituent affects the enzyme potency at the target site.

In comparing the relative biochemical potency of the top three compounds in Table 1, one can note the approximate 300-fold improvement in potency against the *P. aeruginosa* LpxC enzyme when comparing the simple glycine analog (1) to the *s,s*-threonine analog (CH-12). The enzymatic potency is modestly enhanced by the addition of the tethered morpholine tail even though the extension is outside of the active site and exposed to solvent (CH-90). On a cellular level the addition of the morpholino tail does not enhance *P. aeruginosa* activity but leads to a significant improvement in *E. coli* MIC values.

The activity of the glycine analog (1) may be partially restored by alternate substitutions. The racemic-Ala derivative (2) is four-fold more potent than the glycine analog although not sufficiently active to show cellular activity. Addition of a second methyl (*gem* dimethyl, 3) reduces the activity of the series. The racemic valine (4) analog which builds further into the pocket is considerably more potent than the alanine analog (18-fold). A matched pair of both serine analogs shows the importance of chirality, which has previously been noted.¹⁵ The more potent enantiomer is similar in potency to the valine analog in both biochemical and cellular activity despite the change in polarity. Compound 7, an amine, displays similar activity to the valine and serine analogs which is interesting given the change in H-bonding nature of these functional groups.

A series of unnatural amino acids were then evaluated as linkers, this included methionine and phenyl glycine based analogs. Compound 9, the sulfone, showed a marked improvement in biochemical potency over the methionine itself, this may be the result of the formation of an H-bond between the sulfone and Lys238. The addition of an additional α -methyl group to the methionine analog 8 was detrimental to the biochemical activity (data not shown), as was observed in comparing compounds 2 and 3. Addition of an aryl substituent improves the biochemical potency 70-fold when compared to the glycine based compound; the substitution provides good cellular activity despite both the size and the

Table 1
Amino acid based R¹

| Compd. # | R ¹ | AZ Log D | Paelc ₅₀ (nM) | Pae546 (μM) | Pae545 (μM) | Ecolc ₅₀ (nM) | Eco524 (μM) | Eco523 (μM) |
|----------|---|----------|--------------------------|-------------|-------------|--------------------------|-------------|-------------|
| CH-90 |  | 2.3 | 0.6 | <0.2 | 1.6 | 0.2 | <0.2 | <0.2 |
| CH-12 |  | 2.5 | 1.6 | <0.2 | 1.6 | 1 | <0.2 | 1.6 |
| 1 |  | 2.1 | 516 | 12 | >200 | 148 | 12.5 | 100 |
| 2 |  | 2.8 | 128 | 12 | >200 | 19 | 6.3 | 25 |
| 3 |  | 3.3 | 2067 | 100 | >200 | 219 | 50 | 100 |
| 4 |  | 3.3 | 7.1 | 0.8 | 25 | 3.1 | <0.2 | 6.3 |
| 5 |  | 2.0 | 5.3 | 0.8 | 12 | 1.6 | 0.8 | 6.3 |
| 6 |  | 2.2 | 187 | 50 | >200 | 206 | 50 | >200 |
| 7 |  | 1.8 | 28 | 1.6 | 12 | 15 | 1.6 | 6.3 |
| 8 |  | 3.1 | 9.8 | 0.8 | 25 | 1.8 | 0.8 | 6.3 |
| 9 |  | 2.4 | 7.3 | 0.8 | >200 | 1.8 | 0.8 | 6.3 |
| 10 |  | 3.8 | 7.4 | 0.8 | 12 | 2 | 0.4 | 3.2 |
| 11 |  | 3.4 | 80 | 2.5 | >200 | 14 | 3.2 | 12.5 |
| 12 |  | 2.1 | 35 | 1.6 | >200 | 1.6 | 0.8 | 6.3 |

lipophilic character of the group. The less active phenyl glycine enantiomer is still more potent than the glycine analog (**10** vs **11**). Substitution with a more polar aromatic group, imidazole (**12**), resulted in similar binding but a reduced AZ Log D, this substitution unfortunately also increased efflux in *P. aeruginosa* but resulted in no change in *E. coli*.

In general the MIC's against the pump deficient strains of *P. aeruginosa* are less active than those observed in *E. coli*, which may be due to the difference in number, types and expression levels of efflux pumps or cell membrane composition for the two pathogens.

Glutamine analogs: A series of amides which can access further into the pocket and maintain flexibility was designed and evaluated. It was noted in an early survey of amino acid substitutions that the Gln analog (**13**) had good biochemical potency, the physical properties of this compound were also attractive: protein binding, solubility, and calculated Log D. Having established the role of amide in binding with Lys238, additional substitutions were explored to further enhance binding affinity. Amide substitutions were evaluated and all of the analogs showed weaker IC₅₀ values than the initial compound (**13**), although all compounds in this series maintained the attractive physical properties of the lead. A crystal structure of compound **14** was obtained in the *P. aeruginosa* LpxC enzyme which was used in the design of additional analogs (Table 2).

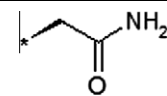
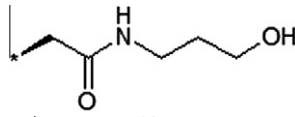
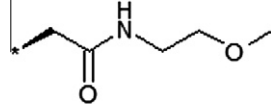
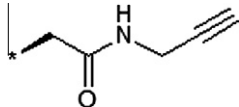
Structural analysis: The wild-type *P. aeruginosa* LpxC structure co-complexed with compound **14** was solved to 2.0 Å resolution.¹⁶ Each asymmetric unit contained two nearly identical monomers (0.27 rsm) with the previously observed β-α-α-β sandwich fold formed by two domains of α-helix and β-sheet layers against each

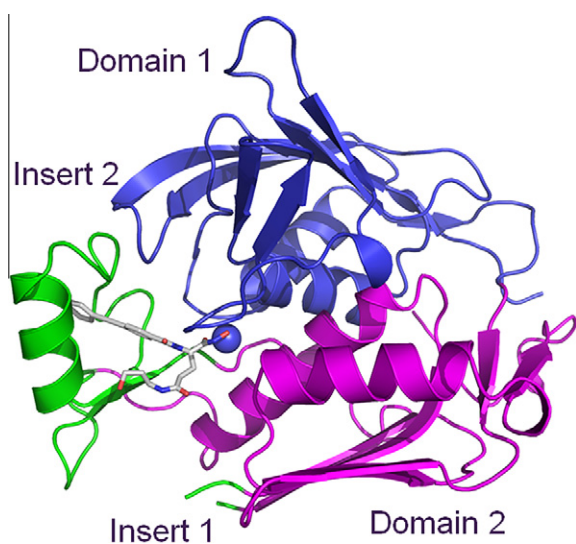
other (Fig. 2).¹⁷ Domain II contains insert regions (Insert I and Insert II) that form the active site pocket. Of these, Insert I is a loop forming a part of the UDP-binding region, while Insert II, which is critical to the inhibitor binding, forms a hydrophobic tunnel with a β-α-β structure that stabilizes the substrate. The active site, in the bottom of Insert II, is comprised of zinc coordinated with His78, His237 and Asp241. A second, non-catalytic zinc atom was identified in the crystal structure (not shown) which is likely a result of the crystallization conditions. The residues from Insert I (residues 160–169) were not defined in the electron density hence are not included in the final structural model.

Compound **14** contains three separate components that contribute to enzyme potency. The hydroxamate coordinates with the catalytic zinc in trigonal bipyrimidyl geometry. This five-coordinate complexation with zinc is similar to other known LpxC inhibitors¹⁸, such as **CH-90**,¹⁷ **BB-78485**,¹⁹ and others.¹⁷ In the crystal structure of compound **14** the hydroxyl amine occupies an axial position and the carbonyl of the hydroxamate is in the equatorial position (Fig. 3). The hydroxamate hydroxyl is located 2.4 Å from the Glu77 acid side chain and the hydroxamate amine is 3.0 Å from the Met62 backbone oxygen. The hydroxamate carbonyl is 2.7 Å from the Thr191 side chain. These three interactions in addition to the metal chelation contribute to the strong potency of the hydroxamate group.

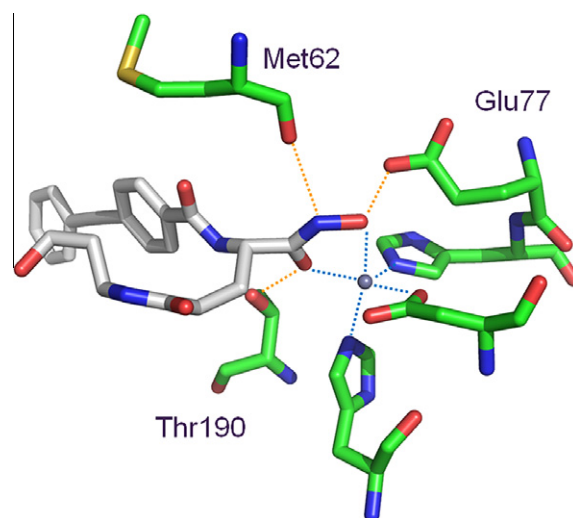
Compound **14** has a hydroxypropyl substituted by a Gln amide in the R¹ position. This group was designed to form hydrogen bonds to residues within the binding pocket occupied by the UDP group of the natural substrate.²⁰ In Figure 4a, the modeled substrate in LpxC forms two hydrogen bonds between the Lys238 and phosphate groups. To mimic the Lys238 interactions, com-

Table 2
Glutamine based linkers.

| Compd # | R ¹ | AZ Log D | PaeIC ₅₀ (nM) | Pae546 (μM) | Pae545 (μM) | EcolC ₅₀ (nM) | Eco524 (μM) | Eco523 (μM) |
|---------|---|----------|--------------------------|-------------|-------------|--------------------------|-------------|-------------|
| 13 |  | 1.3 | 4.4 | 4.4 | >200 | 11 | 2.2 | 35.4 |
| 14 |  | 2.1 | 5.3 | 5.3 | 200 | 1.3 | 3.2 | 50 |
| 15 |  | 2.6 | 33 | 33 | 50 | 3.6 | 1.6 | 25 |
| 16 |  | 2.7 | 14 | 14 | 50 | 4 | 0.8 | 12.5 |

**Figure 2.** Overall structure of LpxC with compound **14**. Shown are Domain I (blue), Domain II (magenta), and two insert regions (green). Residues 160–169 of Insert I was unable to be solved, located at the lower portion of the figure.

pounds with ethylene linked amides were designed (compound **13–16**). Previous docking in a Pae homology model predicted the formation of a hydrogen bond between Lys238 and the amide carbonyl. In the crystal structure, a hydrogen bond occurs between the Lys side chain and the carbonyl, with a distance of 2.7 Å (Fig. 4b). Furthermore, the crystal structure shows hydrophobic interactions between the Phe191 sidechain and ethylene linker due to the stereochemistry of the compound, likely contributing to the 5 nM *P. aeruginosa* IC₅₀ value. The hydroxypropyl group attached to the amide was designed to form hydrogen bonds with the Asp196 side chain and Phe193 backbone amine. The structure shows a hydrogen bond between the hydroxyl and Asp196 side chain (2.6 Å) but not between the hydroxyl and Phe193 backbone amine. This hydroxyl–Asp196 hydrogen bond found in the compound **14** structure could explain the sixfold improvement in the *P. aeruginosa* IC₅₀ over compound **15** which cannot form this hydrogen bond (Fig. 4c). However, the *P. aeruginosa* IC₅₀ value for the unsubstituted amide (compound **13**) is 4.4 nM, illustrating that

**Figure 3.** Residue and ligand interactions with hydroxamate. Hydroxamate forms two metal chelations and each heteroatom interacts with the protein.

hydrogen bonding in the Asp196 region of the active site requires further optimization to improve the potency over compound **13**.

The third essential motif contributing to enzyme potency is the amide/biphenyl acetylene for compound **14**. This portion of the molecule forms both hydrophobic and hydrophilic interactions. The amide nitrogen is within hydrogen bonding distance to Thr190 in the crystal structure. In contrast, the amide carbonyl cannot make any additional H-bonds. The phenyl-acetylene-phenyl group extends into a hydrophobic tunnel and is surrounded by many non-polar side chains including Leu18, Gly192, Ile197, Leu200, Ala206, Gly209, Ala214, and Val216 (Fig. 5). The outer phenyl ring is 15° out of plane with the interior phenyl group to conform to the shape of the hydrophobic tunnel.

The last substitution to be evaluated was based on compound **3** in which the amino acid utilized in the design was disubstituted. Compound **3** was found to be 30-fold less active than the alanine analog (**2**). We had noted that the addition of an additional alpha substitution in the methionine series also reduced enzyme inhibition (data not shown). Could a cyclic R¹ substituent restore activity and provide some rigidity to the substitution? The carbocyclic

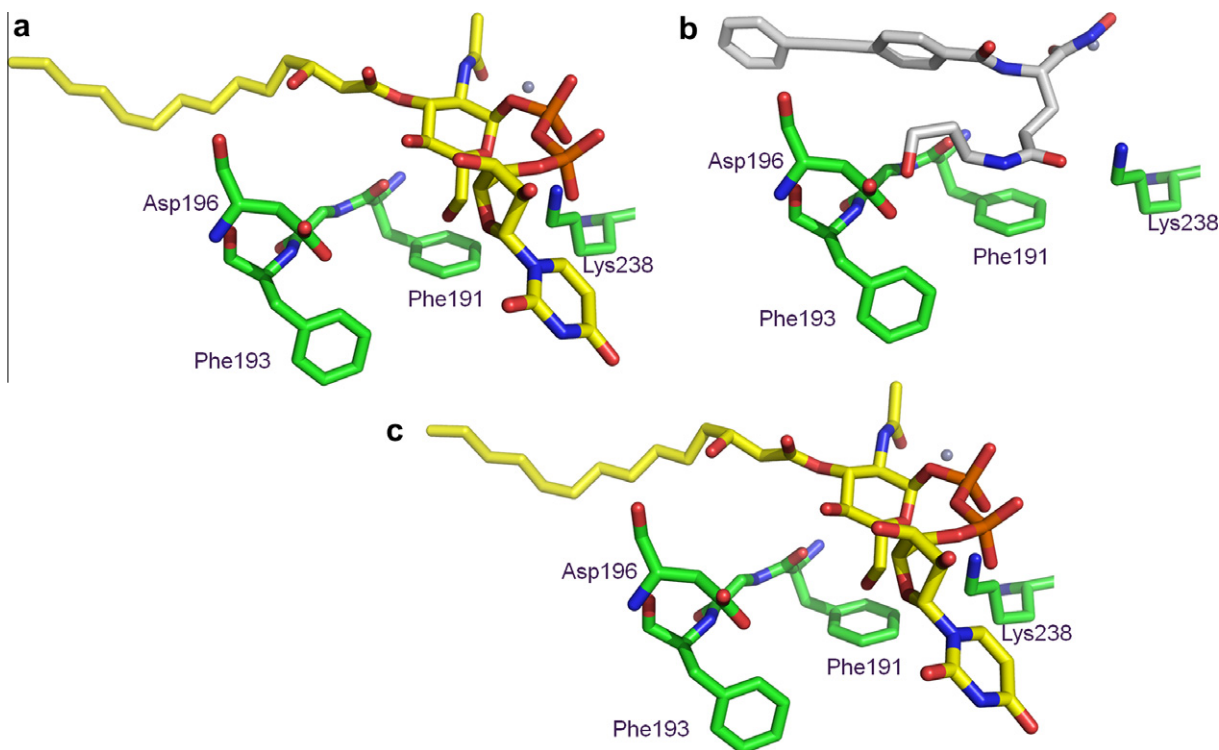


Figure 4. (a) The modeled substrate has two interactions with Lys238. (b) The crystal structure of compound **14** has hydrogen bonds with Lys238 and Asp196. (c) Compound **21** docked in Pae are predicted to hydrogen bond with Lys238.

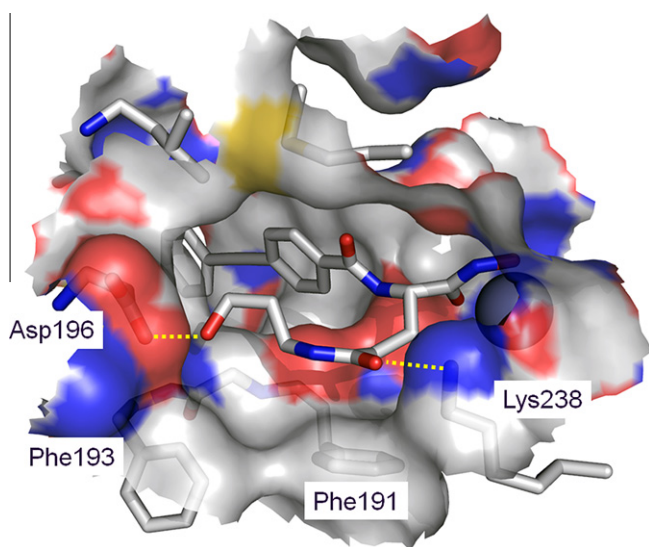


Figure 5. The amide and phenyl-acetylene-phenyl hydrophobic tails of compound **14** form polar and nonpolar interactions with the protein. Seven nonpolar side chains surround the hydrophobic tunnel.

series as initially represented by compounds **17** and **18** were quite similar in potency to compound **3**, but when an acceptor heteroatom was added on the far side of the cyclic substituents the enzymatic potency improved 3 to 10-fold for *O*, *S* and an *N*-benzyl analogs. The most significant improvement resulted from the conversion of compound **20** to the sulfone which has the potential for forming a hydrogen bond with Lys238 as was noted with the Gln amides. This modification showed an additional 10-fold improvement and has the most potent biochemical potency of the cyclic

amino acids evaluated. The smaller and positively charged piperidine analog (**22**) was found to be significantly weaker than the other compounds in this series perhaps due to the proximity to Lys238 (Table 3).

We have designed and prepared a series of amino acid linked analogs using the **CH-12** scaffold as a template to evaluate the potential for improved potency at both enzymatic and cellular levels by building into the UDP pocket. The UDP region of *P. aeruginosa* LpxC substrate binding site is relatively unexplored with respect to inhibitor development.²¹ These efforts were guided by both computational design and structural input to probe the UDP portion of the LpxC pocket. Substituents with a variety of stereochemistry and chemical diversity were utilized to study their impact. The small substituted aliphatic amino acids; alanine, serine and amine based linkers were all well tolerated in the base of the UDP pocket. This study included a series of matched pairs demonstrating strong preference for stereochemistry at the R¹ position. We were able to replace the threonine with methionine, phenylglycine and glutamine based analogs and maintain enzymatic activity, but not maintain cellular activity and physical properties. The glutamine analogs were among the most potent (IC₅₀) in this series and retained desirable physical properties. A co-crystal structure of compound **14** bound to the wild-type LpxC *P. aeruginosa* was obtained and utilized for the design of many of the analogs presented. The structure revealed a hydrogen bond between Lys238 and provided a foundation for further potency improvements by extending into the UDP pocket. The biochemical potency was maintained but not improved in comparison to **CH-12**, with glutamine and sulfone based UDP substitutions offering the most promise for continued exploration. The whole cell activity of the compounds made did not improve in the pump deficient or WT cellular activity when compared to **CH-12**, likely as a function of reduced biochemical activity and increased efflux. Both series were designed to utilize interactions with Lys238. Additional compounds which target improvements in potency through building into the UDP pocket are in progress.

Table 3
Cyclic amino acid based linkers.

| Compd # | R ¹ | AZ Log D | PaelC ₅₀ (nM) | Pae546 (μM) | Pae545 (μM) | EcolC ₅₀ (nM) | Eco524 (μM) | Eco523 (μM) |
|---------|--|----------|--------------------------|-------------|-------------|--------------------------|-------------|-------------|
| 17 |  | 3.1 | 8100 | 200 | >200 | 178 | 50 | >200 |
| 18 |  | 3.8 | 3500 | 100 | >200 | 98 | 6.3 | 100 |
| 19 |  | 2.2 | 334 | 50 | >200 | 12 | 6.3 | 50 |
| 20 |  | 3.0 | 296 | 12.5 | >200 | 22 | 1.6 | 25 |
| 21 |  | 2.1 | 26 | 25 | 100 | <4 | 0.8 | 50 |
| 22 |  | 0.8 | 11000 | 200 | >200 | 102 | 50 | >200 |
| 23 |  | 3.4 | 208 | 25 | >200 | 3434 | 3.2 | 12.5 |

Acknowledgements

We would like to thank Maria Uria-Nickelsen for her helpful suggestions and feedback on the document. We would also like to acknowledge contributions from Senthilkumar Kuppusamy and the chemists at Syngene.

Supplementary data

Supplementary data associated with this article can be found, in the online version, at <http://dx.doi.org/10.1016/j.bmcl.2013.02.055>.

References

- Vergidis, P. I.; Falagas, M. E. *Curr. Opin. Invest. Drugs* **2008**, *9*, 176.
- (a) Nikaïdo, H.; Vaara, M. *Microbiol. Rev.* **1985**, *49*, 1–32; (b) Doerrler, W. T. *Mol. Microbiol.* **2006**, *60*, 542; (c) Sperandio, P.; Deho, G.; Polissi, A. *Biochim. Biophys. Acta* **2009**, *1791*, 594.
- (a) Anderson, M. S.; Bull, H. S.; Galloway, S. M.; Kelly, T. M.; Mohan, S.; Radhika, K.; Raetz, C. R. H. *J. Biol. Chem.* **1993**, *268*, 19858; (b) Beall, B.; Lutkenhaus, J. J. *Bacteriology* **1987**, *169*, 5408.
- (a) Jackman, J. E.; Fierke, C. A.; Tumeý, L. N.; Pirrung, M.; Uchiyama, T.; Tahir, S. H.; Hindsgaul, O.; Raetz, C. R. H. *J. Biol. Chem.* **2000**, *275*(15), 11002; (b) Raetz, C. R. H.; Guan, Z. Q.; Ingram, B. O.; Six, D. A.; Song, F.; Wang, X. Y.; Zhao, J. S. *J. Lipid Res.* **2009**, *50*, S103; (c) Wang, X.; Quinn, P. *Prog. Lipid Res.* **2010**, *49*, 97.
- Williams, A. H.; Raetz, C. R. H. *Proc. Natl. Acad. Sci. U.S.A.* **2007**, *104*(34), 13543.
- Raetz, C. R. H., 2nd ed. In *Escherichia coli and Salmonella: Cellular and Molecular Biology*; Neidhardt, F. C., Ed.; American Society for Microbiology: Washington, DC, 1996; *1*, p 1035.
- (a) Gomez, M.; Hackbarth, C.; Rafanan, N.; Kubo, A.; Wang, W.; Tembe, V.; Margolis, P.; Chen, D.; O'Dowd, H.; Raju, B.; Yuan, Z.; Patel, D. WO2011005355; (b) White, R.; Trias J. *Intersci. Conf. Antimicrob. Agents Chemother*, Sep 27–30, 2002; 42: abstract F-2034.
- (a) Onishi, H. R.; Pelak, B. A.; Gerckens, L. S.; Silver, L. L.; Kahan, F. M.; Chen, M.-H.; Patchett, A. A.; Galloway, S. M.; Hyland, S. A.; Anderson, M. S.; Raetz, C. R. H. *Science* **1996**, *274*, 980; (b) Warmus, J. S.; Quinn, C. L.; Taylor, C.; Murphy, S. T.; Johnson, T. A.; Limberakis, C.; Ortwine, D.; Bronstein, J.; Pagano, P.; Knafels, J. D.; Lightle, S.; Mochalkin, I.; Brideau, R.; Podoll, T. *Bioorg. Med. Chem. Lett.* **2012**, *22*(7), 2536.
- (a) Coggins, B. E.; Li, X.; McClerren, A. L.; Hindsgaul, O.; Raetz, C. R. H.; Zhou, P. *Nat. Struct. Biol.* **2003**, *10*, 645; (b) Whittington, D. A.; Rusche, K. M.; Shin, H.; Fierke, C. A.; Christianson, D. W. *Proc. Natl. Acad. Sci. U.S.A.* **2003**, *100*, 8146.
- Anderson, N. H.; Bowman, J.; Erwin, A.; Harwood, E.; Kline, T.; Mdluli, K.; Ng, S.; Pfister, K. B.; Shawar, R. I.; Wagman, A.; Yabannavar, A. WO2004062601 A2, see example 12 (CH-12).
- Anderson, N. H.; Bowman, J.; Erwin, A.; Harwood, E.; Kline, T.; Mdluli, K.; Ng, S.; Pfister, K. B.; Shawar, R. I.; Wagman, A.; Yabannavar, A. WO2004062601 A2, see example 83 (CH-90).
- For more detailed information on IC 50 assays, cell lines used in microbiology and AZ log D and PPB methods see supplementary material.
- MIC (Minimum Inhibitory Concentration) measurements performed according to Clinical and Laboratory Standards Institute, Wayne, PA on the following bacterial strains from the AstraZeneca collection: *P. aeruginosa* ARC545, *P. aeruginosa* toIC-ARC546, *Escherichia coli* ARC523 and *E. coli* toIC-ARC524.
- Bruneau, P.; McElroy, N. R. *J. Chem. Inf. Model.* **2006**, *46*, 1379.
- Liang, X.; Lee, C.-L.; Chen, X.; Chung, H. S.; Zeng, D.; Raetz, C. R. H.; Li, Y.; Zhou, P.; Toone, E. J. *Bioorg. Med. Chem.* **2011**, *19*, 852.
- The structure and is deposited in the Protein Data Bank (PDB) as 4J3D, *Pseudomonas aeruginosa* LpxC in complex with a hydroxamate inhibitor.
- Barb, A. W.; Jiang, L.; Raetz, C. R. H.; Zhou, P. *Proc. Natl. Acad. Sci. U.S.A.* **2007**, *104*, 18433.
- (a) Gennadios, H. A.; Whittington, D. A.; Li, X.; Fierke, C. A.; Christianson, D. W. *Biochemistry* **2006**, *45*, 7940; (b) Coggins, B. E.; McClerren, A. L.; Jiang, L.; Li, X.; Rudolph, J.; Hindsgaul, O.; Raetz, C. R. H.; Zhou, P. *Biochemistry* **2005**, *44*, 1114.
- Mochalkin, I.; Knafels, J. D.; Lightle, S. *Protein Sci.* **2008**, *17*, 450.
- Gennadios, H. A.; Christianson, D. W. *Biochemistry* **2006**, *45*, 15216.
- Warmus, J. S.; Quinn, C. L.; Taylor, C.; Murphy, S. T.; Johnson, T. A.; Limberakis, C.; Ortwine, D.; Bronstein, J.; Pagano, P.; Knafels, J. D.; Lightle, S.; Mochalkin, I.; Brideau, R.; Podoll, T. *Bioorg. Med. Chem. Lett.* **2012**, *22*, 2536.